Acta Oceanologica Sinica 2008, Vol. 27, No. 3, p. 79~87
http://www.oceanpress.com.cn
E-mail: hyxbe@263.net

Observations and modeling of the ice-ocean conditions in the coastal Chukchi and Beaufort Seas

JIN Meibing[1*], WANG Jia[2], MIZOBATA Kohei[3], HU Haoguo[4], SHIMADA Koji[3]

1. International Arctic Research Center, University of Alaska Fairbanks, AK 99775—7340, USA
2. NOAA, Great Lakes Environmental Research Laboratory, Ann Arbor, MI 48105, USA
3. Tokyo University of Marine Science and Technology, 4—5—7 Kounan, Minato-ku Tokyo, 108—8477, Japan
4. Cooperative Institute for Limnology and Ecosystems Research, School of Natural Resources and Environment, University of Michigan, Ann Arbor, MI, USA

Received 15 August 2007; accepted 27 February 2008

Abstract

The Chukchi and Beaufort Seas include several important hydrological features: inflow of the Pacific water, Alaska coast current (ACC), the seasonal to perennial sea ice cover, and landfast ice along the Alaskan coast. The dynamics of this coupled ice-ocean system is important for both regional scale oceanography and large-scale global climate change research. A number of moorings were deployed in the area by JAMSTEC since 1992, and the data revealed highly variable characteristics of the hydrological environment. A regional high-resolution coupled ice-ocean model of the Chukchi and Beaufort Seas was established to simulate the ice-ocean environment and unique seasonal landfast ice in the coastal Beaufort Sea. The model results reproduced the Beaufort gyre and the ACC. The depth-averaged annual mean ocean currents along the Beaufort Sea coast and shelf break compared well with data from four moored ADCPs, but the simulated velocity had smaller standard deviations, which indicate small-scale eddies were frequent in the region. The model results captured the seasonal variations of sea ice area as compared with remote sensing data, and the simulated sea ice velocity showed an almost stationary area along the Beaufort Sea coast that was similar to the observed landfast ice extent. It is the combined effects of the weak oceanic current near the coast, a prevailing wind with an onshore component, the opposite direction of the ocean current, and the blocking by the coastline that make the Beaufort Sea coastal areas prone to the formation of landfast ice.

Key words: circulation, sea ice, fast ice, Beaufort Sea, coupled ice-ocean model

1 Introduction

The Chukchi and Beaufort Seas include the vast Chukchi Sea shelf (≈50 m depth), and the Beaufort Sea shelf and its extension to the basin (see Fig. 1). The physical oceanography of the Chukchi and Beaufort Seas is featured by seasonal to perennial sea ice cover, and interactions of several important water masses: the incoming warm and fresh Pacific water, the cold and salty arctic surface water, and the Atlantic intermediate water (Weingartner et al., 2006; Pickart et al., 2005; Weingartner et al., 1998). The

Foundation item: We acknowledge the support provided by the Minerals Management Service and the Coastal Marine Institute of University of Alaska Fairbanks project 2004-061. We would also like to acknowledge support from the International Arctic Research Center (IARC) of the University of Alaska Fairbanks and Japan Marine Science and Technology Center (JAMSTEC) and the mooring data from JAMSTEC. This is GLERL Contribution No. 1466.
* Corresponding author, E-mail: mjin@iarc.uaf.edu

minimum ice extent and ice edge of the arctic that usually fall in this area have been widely used as indicators of global climate change (Stroeve et al., 2005). Regionally, the Alaskan coastal landfast ice is a key element of the Alaskan coastal system, integral to a wide range of geological and biological processes as well as human activities. Along the coast of the Alaskan arctic, landfast sea ice can extend from 18 to 30 m water depth in the winter months in the Beaufort Sea (Stringer et al., 1980). It provides seasonal access from the land to hunting grounds at its seaward edge and is utilized as a platform for offshore oil development. Its presence can mitigate the effect of winter storms on the coast. Alaskan landfast ice is typically a seasonal phenomenon. Its annual cycle can be broadly characterized by a gradual seaward advance from the coast beginning in early winter followed by a rapid retreat coinciding with the onset of spring (Mahoney, Eicher, Gaylord et al., 2007).

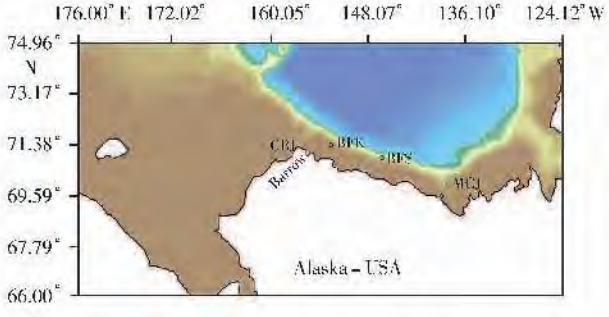

Fig. 1. Model domain with colors indicating water depth from less than 100 m in the shelf to more than 3 000 m in the basin, and locations of mooring CBJ, BFK, BFS and MCJ.

Although a great effort of coupled ice-ocean modelling has covered this important area, most of these regional-to-global models tend to have coarse resolutions of being approximately 20 to 100 km (Holloway et al., 2007; Wang et al., 2005) and have a focus on the large-scale phenomena of the Arctic Regions or larger areas. The small-scale phenomena, such as the Alaskan coastal current and landfast ice, are barely resolved in those models. Besides the resolution, the mechanism of the formation of landfast ice in different regions was not well identified due to limited observations, and the methods to simulate the fast ice in the sea – ice model were not yet developed and tested in different coastal ice- ocean systems. These locally important features in the coastal areas have to be simulated with adequately high-resolution models and thus, their contribution to the large-scale circulation can be assessed. The demands from the coastal community, offshore oil industry, navigation and transportation, and growing international interests in the climate change in the polar region, are the main incentives for this study. The high-resolution coupled 3-D ice – ocean model of the Chukchi and Beaufort Seas was developed to understand and simulate the main dynamics of the complicated ice – ocean system. Instead of discussing every aspect of the coupled ice – ocean model results, we focused on the ocean current and sea ice area in the Alaska coastal region and their relation to the formation of landfast ice along the Beaufort Sea coast. Presented below are the observational data used in the study, the coupled ice – ocean model settings, and a discussion on the model-data comparisons.

2 Observations

Most of the observations in the areas were mainly conducted during arctic expeditions from various countries in the summer (July to September). The long ice-covered winter conditions are mainly observed through moorings (Woodgate et al., 2005a) and some rare submarine measurements, e. g., scientific ice expeditions (SCICEX 99) of the US Navy from 1995 to 1999. In this study, four out of 16 moorings deployed by the Japan Marine Science and Technology Center (JAMSTEC) between 1992 and 2000 were chosen because of their representative locations along the Alaskan coast (mooring locations in Fig. 1). The time interval and depth range of the

moorings are shown in Table 1. Each mooring includes at least one full annual cycle of the hydrological variables, such as CTD temperature and salinity, and ADCP current data at several depth levels. Large-scale sea – ice concentrations from the National Snow and Ice Data Center's (NSIDC) remote sensing data measured by special sensor microwave/imager (SSM/I, 20 km resolution) are interpolated into our model grid for comparison. Monthly climatology of the Beaufort Sea coastal landfast ice is from Mahoney, Eichen, Gaylord et al. (2007) based on their multiyear SAR observations and data analysis.

Table 1. JAMSTEC mooring names, time interval, bottom depth, and ADCP instrument depth

Station name	Time interval	Bottom depth/m	Instrument depth/m
CBJ	Sep. 1992 Jul. 1997	75	10 ~ 56
BFK	Jul. 1998 Oct. 1999	132	82 ~ 126
BFS	Jul. 1998 Oct. 1999	513	101 ~ 250
MCJ	Oct. 1999 Oct. 2000	260	164 ~ 243

3 Coupled ice – ocean model

The coupled ice – ocean model (CIOM, Wang et al., 2005; Yao et al., 2000) consists of a multicategory sea ice model (Hibler, 1980, 1979) and the Princeton ocean model (POM, Mellor, 1996; Blumberg and Mellor, 1987). The CIOM has been applied to the Pan-Arctic Atlantic Ocean with a horizontal resolution of 27.5 km (Wang et al., 2005). The model was reconfigured for this study, and the model domain (Fig. 1) was large enough to include most of the circulation features in the Chukchi and Beaufort Seas, such as the inflow of North Pacific water from the Bering Strait, the Beaufort gyre in the Canada Basin, and the intrusion of intermediate water from the North Atlantic through open boundary fluxes. The open boundary conditions of oceanic and sea ice fluxes are from a coupled global ice-ocean model [(1/6)° meridional by (1/4)° zonal] by the Center for Climate System Research (CCSR), University of Tokyo (Holloway et al., 2007; Watanabe et al., 2006). This global model is one of the Intergovernmental Panel on Climate Change (IPCC) models. The transport through the Bering Strait was also modified with the observational data by Woodgate et al. (2006, 2005b), and the total transport along all open boundaries were adjusted accordingly to reach a balance at each time step.

To resolve the important coastal current and eddy activities along the shelf break of the Beaufort Sea (Manley and Hunkins, 1985), the coupled ice-ocean model was configured with a high resolution to simulate the ice and ocean dynamics. The horizontal resolution of (1/28)° by (1/8)° (3.9 km in meridinal direction and 3.8 ~ 5.6 km in zonal direction from the north to the south boundaries) is less than the first baroclinic Rossby radius of deformation of about 21.5 km (Shaw and Chao, 2003) in the region. Tidal current is not included in this study, because the Beaufort Sea tidal current is very weak (as shown later from the ADCP data), on the order of 1 cm/s or less in most regions, much less than other Beaufort Sea coastal and wind-driven currents.

The model runs from 1990 to present with daily atmospheric forcing data (wind, air temperature, air specific humidity, and precipitation) from the National Center for Environmental Protection (NCEP) reanalysis data set, following Wang et al. (2005). Initial temperature and salinity are interpolated from the Polar Science Center hydrographic climatology

(PHC 3.0, Steele et al., 2001).

4 Results and discussion

4.1 Comparison of model results with mooring data

The model results of 1999 were used for comparisons with the mooring data because most of the data were from 1998 to 1999 (see Table 1). The simulated annual mean depth-averaged (over the depth range of the mooring data) current vector at the four stations (Fig. 2) showed good agreement with the observations in both direction and magnitude. These vectors represent the mean circulation patterns in the coastal Chukchi and Beaufort Seas: the coastal current was strong and persistent (annual mean of 28 cm/s and standard deviation of 21 cm/s calculated from the monthly mean data) in the Barrow Canyon because of the narrow topography effects; the current was weaker and unstable (annual mean of 3.8 ~ 5.8 cm/s and standard deviation of 2.3 ~ 6.1 cm/s) at stas BFK and BFS after turning into the Beaufort Sea, and only 1 cm/s at Sta. MCJ. But the weak current at those Beaufort Sea moorings was also because these stations are on the edge of the shelf and the shelf break, where two opposite circulation patterns in the Beaufort Sea meet: (1) the ACC that flows eastward along the Beaufort Sea coast, and (2) the Beaufort gyre that flows westward along the shelf break. Those two current patterns were present in both fully ice-covered winter months (Fig. 3a) and in the summer months (Fig. 3b) when the coastal ice was melted. The ACC was maintained by strong freshwater input along the Alaska coast and

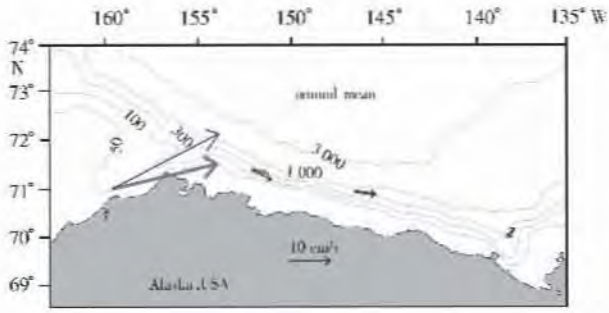

Fig. 2. Comparison of simulated and observed annual mean depth-averaged current at the four mooring stations.

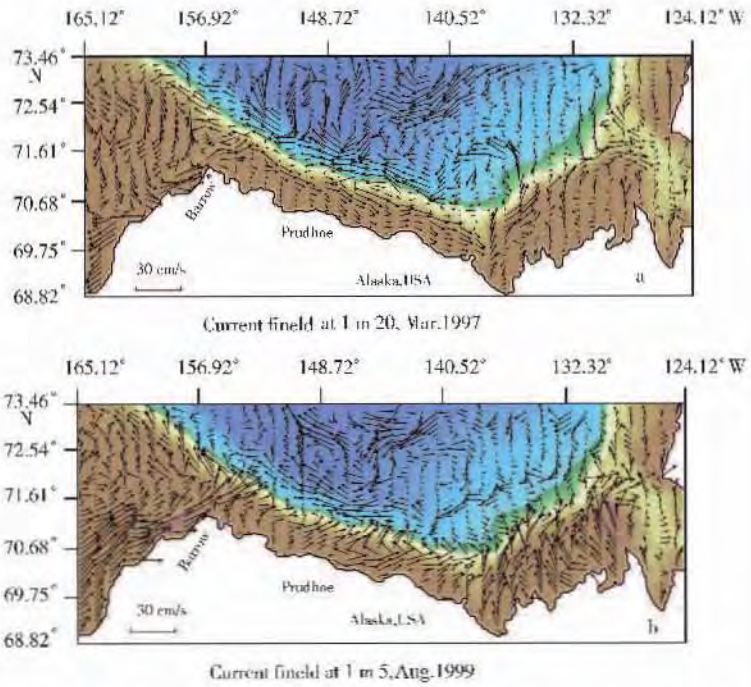

Fig. 3. Modeled sea surface (at 1 m depth) current field imposed on topography. The arrows in red denote velocities greater than 30 cm/s.

was opposite to the annual mean wind in the Beaufort Sea (see Fig. 4) that maintained the Beaufort gyre. Although the annual mean wind speed was very small (2 ~ 5 m/s), occasional storms can produce strong disturbance to the weak mean current system. The power spectrum of the ADCP data from Sta. BFK (see Fig. 5) showed almost continuous energy signals in the 1 h to 1 d period. The semidiurnal and diurnal tidal energy was weak and unidentifiable in the spectrum. The simulated current at Sta. BFK showed smaller and lesser high-frequency variance than the observed velocities (see Fig. 6), although the annual mean is very close (see Fig. 2). Since the high-frequency movement has much lower energy compared with long-term mean current in the power spectrum, the model results can still represent the main dynamics of the ocean current. Those high-frequency activities indicate that short-time and small-scale events, such as internal waves, eddies and cyclones etc., were frequent in the region and more efforts are needed to understand their mechanism and include them in the model.

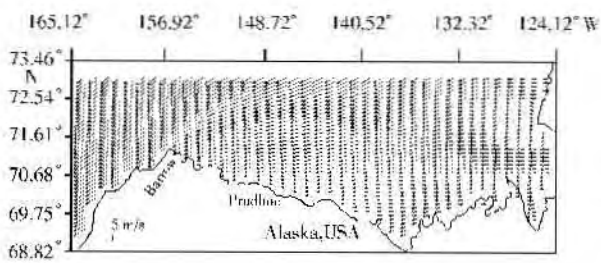

Fig. 4. Annual mean wind of 1999 from NCEP reanalysis data.

4.2 Comparison of model results with sea ice observations

Most of the sea ice on the Beaufort and Chukchi Seas shelves is seasonal ice that starts to form quickly from north to south in October, but the melting of the sea ice usually takes much longer from south to north in June to mid-September. The modelled sea ice area (Fig. 7) showed such an annual cycle and

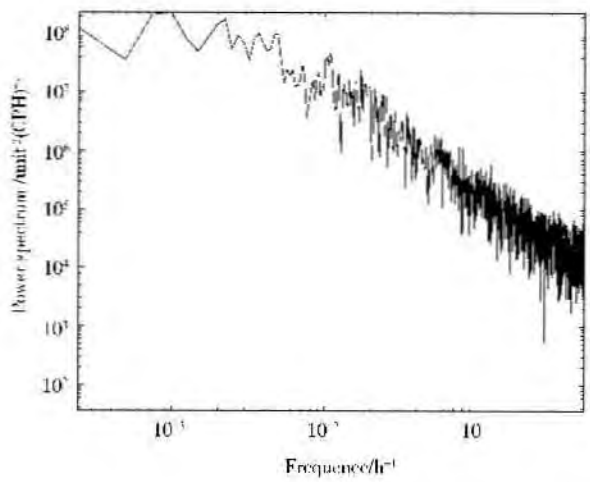

Fig. 5. Specturm of the ADCP velocity at BFK station (CPH denotes cycle per hour).

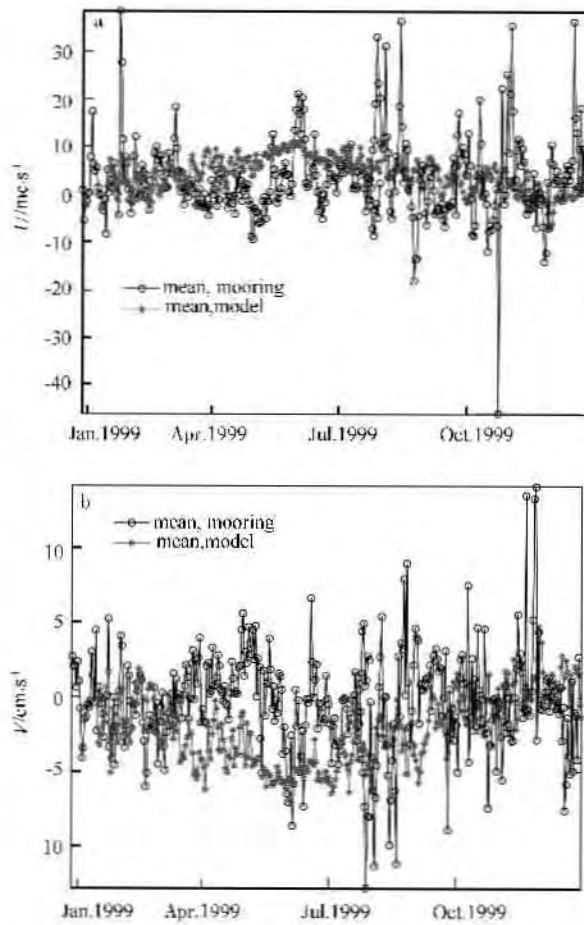

Fig. 6. Simulated and observed depth-averaged U and V at BFK station.

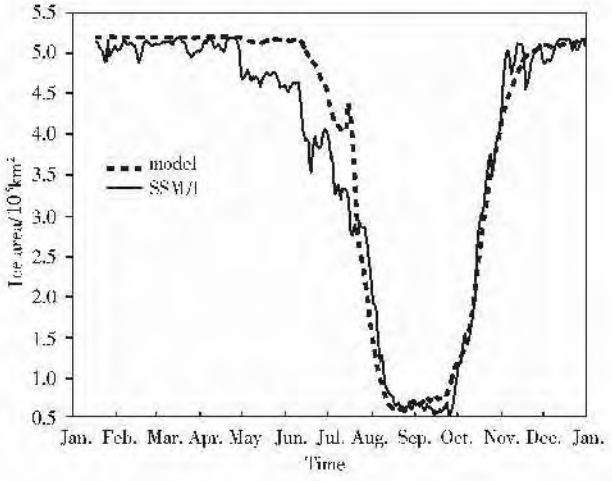

Fig. 7. Comparison of modeled and SSM/I-measured annual cycle of ice area in 1999.

compared well with the SSM/I observations. Here, the total sea ice-covered area was summed for the model and SSM/I data at each grid in the model domain where sea ice concentration was greater than 15% (SSM/I data contains a lot of noise below this level). The simulated ice edge compared reasonably with the SSM/I data in the summer (Fig. 8b).

The sea ice flow fields in both fully sea ice-covered winter season (Fig. 8a) and summer when most of the coastal ice was melted (Fig. 8b) showed a similar Beaufort gyre pattern as the sea surface current (see Fig. 3) in response to wind forcing. But in the winter, the ice flow was weaker than the ocean current in the ACC area, because different directions

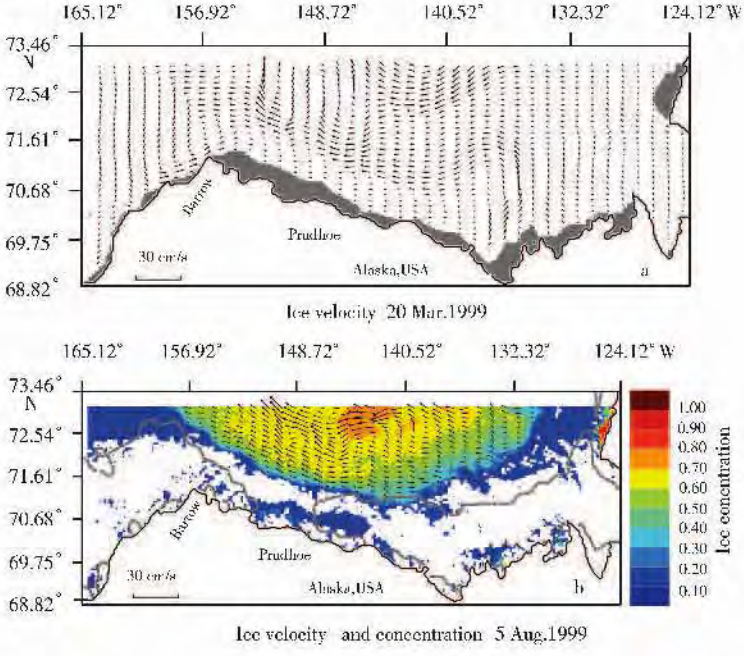

Fig. 8. Modeled ice velocity; shaded areas indicate velocity less than 1 cm/s (a) and comparison of modeled ice concentration and SSM/I ice edge (contour of 15% ice concentration) (b).

of the wind offset part of the ACC drag on the sea ice. Under little external forcing by combined wind and oceanic drag and the blocking effects of the coastline on wind-driven ice drift, the sea ice along the Beaufort Sea coast had become virtually stationary in the model. The shaded areas in Fig. 8a denote areas where sea ice velocities were less than 1 cm/s, and this area is very similar to the observed monthly mean landfast ice in March (Fig. 9, from Mahoney, Eicken et al., 2007). Landfast ice extent in different areas of the arctic is controlled by different mechanisms, e. g., barrier islands and involved coastlines, a lack of strong currents and tides, and shallow water are all conducive to the formation of

landfast ice. Figure 8a suggests that the combined atmospheric-ice-ocean conditions in the coastal Beaufort Sea can produce weak ice flow and, thus, the area is prone to the formation of landfast ice. Since the axis of ACC was further away from the coast in the Beaufort Sea than the Chukchi Sea, the fast ice extent can grow wider along the Beaufort Sea coast. To well resolve the ACC and the narrow strip between the ACC and Beaufort Sea coastline is essential for modelling the Alaskan coastal fast ice.

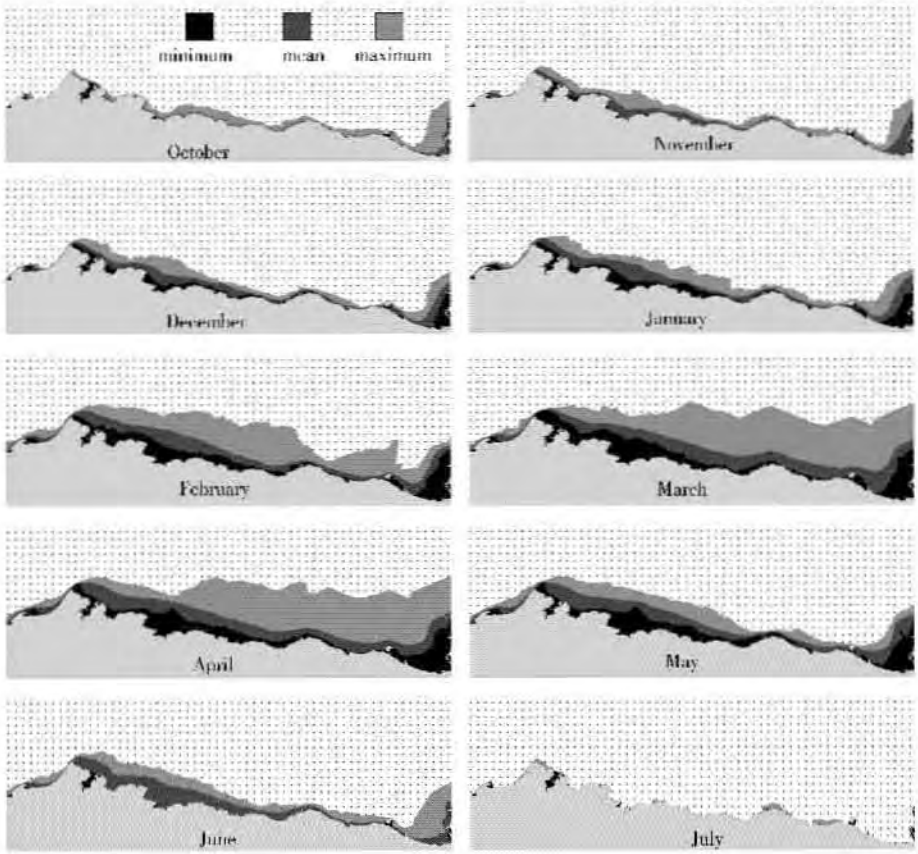

Fig. 9. Minimum mean and maximum monthly mean landfast sea ice extents. The dotted area indicates where land ice was never observed (Mahoney et al., 2006).

There are also other possible mechanisms for landfast ice formation that are still not included in the model, for example, ridges can be formed by the convergence and shear of westward drifting ice in the Beaufort gyre against the coast and local onshore wind (Mahoney et al., 2004), and these events play an important role in anchoring the landfast ice. The anchoring strength provided by ridges could be two to three orders of magnitude greater than typical wind or water stresses (Mahoney, Eicken and Shapiro, 2007). Therefore, additional decoupling processes, such as sea level surges or thermal erosion of keels, must occur in addition to offshore current stress in order to cause the landfast ice to detach. Although the fast ice can cover a large area (see Fig. 9), its scale is heterogeneous in different directions. These anchoring ridges that sometimes were also the edge of the fast ice, could be long in length, but very narrow in width for the current sea ice model to resolve. The ridge thickness in a model grid much coarser than the real ridge scale would be significantly underestimated, and thus, not thick

enough to touch the seafloor. Therefore parameterization of those small-scale dynamics is necessary to include the mechanism in the ice – ocean models.

5 Summary

The Chukchi and Beaufort Seas include the interactions of several important water masses: the incoming warm and fresh Pacific water, the cold and salty arctic surface water, and the Atlantic intermediate water. The current system in the Beaufort Sea is strongly shaped by these water masses. The ACC was strong at the Barrow Canyon, but after it turned into the Beaufort Sea, the ACC was weakened and became unstable under the influence of the Beaufort gyre and the prevailing wind in the opposite direction of the ACC. The observed oceanic current revealed low-energy and high-frequency small-scale activities in the Beaufort Sea. The seasonal variations of the current were also high, and the annual mean oceanic current at the BFK and the BFS on the shelf break were at the same level or less than their standard deviation.

The combined effects of the ocean current, wind, and coastline made the Beaufort Sea coast prone to the formation of the landfast ice. High resolution is essential to simulate this ice ocean condition along the Alaskan coast. Some mechanisms, such as ridges formed by the convergence and shear of drifting ice, have heterogeneous scales in different directions and are too narrow in width for the current sea ice model to resolve. Thus, further parameterization of those small-scale dynamics is necessary in the future to include the mechanism in the ice – ocean models.

References

Blumberg A F, Mellor G L. 1987. A description of a three-dimensional coastal ocean circulation model: three-dimensional coastal ocean model. In: Heaps N S, ed. Coastal Estuarine Science, v4. Washington D C: AGU, 1 ~ 16

Hibler W D. 1979. A dynamic thermodynamic sea ice model. J Phys Oceanogr, 9: 815 ~ 846

Hibler W D, 1980. Modeling a variable thickness sea ice cover. Mon Weather Rev, 108: 1943 ~ 1973

Holloway G, Dupont F, Golubeva E, et al. 2007. Water properties and circulation in Arctic Ocean models. J Geophys Res, 112: C04S03, doi:10.1029/2006JC003642

Mahoney A, Eicken H, Shapiro L, et al. 2004. Ice motion and driving forces during a spring ice shove on the Alaskan Chukchi coast. J Glaciol, 50: 169, 195 ~ 207

Mahoney A, Eicken H, Shapiro L. 2007. How fast is landfast ice? A study of the attachment and detachment of nearshore ice at Barrow, Alaska. Cold Reg Sci Technol, 47: 233 ~ 255

Mahoney A, Eichen H, Gaylord A G, et al. 2007. Alaskan landfast sea ice: links with bathymetry and atmospheric circulation. J Geophys Res, 112: C02001, doi: 10.1029/2006JC003559

Manley T O, Hunkins K. 1985. Mesoscale eddies of the Arctic Ocean. J Geophys Res, 90: 4911 ~ 4930

Mellor G L. 1996. User's Guide for a Three-Dimensional Primitive Equation, Numerical Ocean Model. Atmos and Oceanic Sci Program, Princeton Univ, Princeton, NJ. 53

Pickart R S, Weingartner T, Pratt L J, et al. 2005. Flow of winter-transformed Pacific water into the western Arctic. Deep-Sea Res (Ⅱ), 52 (24 ~ 26): 3175 ~ 3199

Shaw P T, Chao S Y. 2003. Effects of a baroclinic current on a sinking dense water plume from a submarine canyon and heton shedding. Deep-Sea Res (Ⅰ), 50(2003): 357 ~ 370

Steele M, Morley R, Ermold W. 2001. PHC: a global ocean hydrography with a high quality Arctic Ocean. J Clim, 14: 2079 ~ 2087

Stringer W J, Barrett S A, Schreurs L K., 1980. Nearshore Ice Conditions and Hazards in the Beaufort, Chukchi and Bering Seas. Geophysical Institute, University of Alaska, Fairbanks, AK.

Stroeve J C, Serreze M C, Fetterer F, et al. 2005. Tracking the Arctic's shrinking ice cover: another extreme September minimum in 2004. Geophys Res Lett, 32: L04501, doi:04510.01029/02004GL021810

Wang J, Liu Q, Jin M, et al. 2005. A coupled ice – ocean

model inthe pan Arctic and North Atlantic Ocean: simulation of seasonal cycles. J Oceanogr, 61: 213 ~ 233

Watanabe E, Wang J, Sumi T, et al. 2006. Arctic dipole and its contribution to sea ice exports in the last 20th century. Geophys Res Lett, 33: L23703, doi: 10. 1029/2006GL028112

Weingartner T J, Cavalieri D J, Aagaard K, et al. 1998. Circulation, dense water formation and outflow on the northeast Chukchi Sea shelf. J Geophys Res, 103: 7647 ~ 7662

Weingartner T, Aagaard K, Woodgate R, et al. 2005. Circulation on the north central Chukchi Sea Shelf, Deep-Sea Res (Ⅱ), 52(24 ~ 26): 3150 ~ 3174.

Woodgate R A, Aagaard K, Weingartner T. 2005a. A year in the physical oceanography of the Chukchi Sea: moored measurements from autumn 1990—91. Deep-Sea Res (Ⅱ), 52(24 ~ 26): 3116 ~ 3149

Woodgate R A, Aagaard K, Weingartner T. 2005b. Monthly temperature, salinity, and transport variability of the Bering Strait throughflow. Geophys Res Lett, 32(4): doi 10. 1029/2004GL022112, 2005

Woodgate R A, Aagaard K, Weingartner T J. 2006. Interannual changes in the Bering Strait fluxes of volume, heat and freshwater between 1991 and 2004. Geophys Res Lett, 33: L15609, doi:10. 1029/2006GL026931

Yao T, Tang C L, Peterson I K. 2000. Modeling the seasonal variation of sea ice in the Labrador Sea with a coupled multicategory ice model. J Geophys Res, 105:1153 ~ 1165